



BNL-82134-2009-CP

***Material Properties Limiting the Performance of
CZT Gamma-Ray Detectors***

**A.E. Bolotnikov, S. Babalola, G.S. Camarda, Y. Cui,
S.U. Egarievwe, A. Hossain, G. Yang, and R.B. James**

Presented at the 43rd Annual GOMAC Tech Conference
Brookhaven National Laboratory, Upton, NY
March 16-19, 2009

January 2009

Nonproliferation and National Security Department

Brookhaven National Laboratory

P.O. Box 5000
Upton, NY 11973-5000
www.bnl.gov

Notice: This manuscript has been authored by employees of Brookhaven Science Associates, LLC under Contract No. DE-AC02-98CH10886 with the U.S. Department of Energy. The publisher by accepting the manuscript for publication acknowledges that the United States Government retains a non-exclusive, paid-up, irrevocable, world-wide license to publish or reproduce the published form of this manuscript, or allow others to do so, for United States Government purposes.

This preprint is intended for publication in a journal or proceedings. Since changes may be made before publication, it may not be cited or reproduced without the author's permission.

DISCLAIMER

This report was prepared as an account of work sponsored by an agency of the United States Government. Neither the United States Government nor any agency thereof, nor any of their employees, nor any of their contractors, subcontractors, or their employees, makes any warranty, express or implied, or assumes any legal liability or responsibility for the accuracy, completeness, or any third party's use or the results of such use of any information, apparatus, product, or process disclosed, or represents that its use would not infringe privately owned rights. Reference herein to any specific commercial product, process, or service by trade name, trademark, manufacturer, or otherwise, does not necessarily constitute or imply its endorsement, recommendation, or favoring by the United States Government or any agency thereof or its contractors or subcontractors. The views and opinions of authors expressed herein do not necessarily state or reflect those of the United States Government or any agency thereof.

Material Properties Limiting the Performance of CZT Gamma-Ray Detectors

**Aleksey E. Bolotnikov¹, Stephen Babalola^{2,3}, Giuseppe S. Camarda¹,
Yonggang Cui¹, Stephen U. Egarievwe^{1,3}, Anwar Hossain¹, Ge Yang¹,
and Ralph B. James¹**

¹Brookhaven National Laboratory, Upton, NY 11973, USA

²Fisk University, Nashville, TN 37208, USA

³Vanderbilt University, Nashville, TN 37235,

Abstract: *CdZnTe (CZT) nuclear radiation detectors are advanced sensors that utilize innovative technologies developed for wide band-gap semiconductor industry and microelectronics. They open opportunities for new types of room-temperature operating, field deployable instruments that provide accurate identification of potential radiological threats and timely awareness for both the civilian and military communities. Room-temperature radiation detectors are an emerging technology that relies on the use of high-quality CZT crystals whose availability is currently limited by material non-uniformities and the presence of extended defects. To address these issues, which are most critical to CZT sensor developments, we developed X-ray mapping and IR transmission microscopy systems to characterize both CZT crystals and devices. Since a customized system is required for such X-ray measurements, we use synchrotron radiation beams available at BNL's National Synchrotron Light Source. A highly-collimated and high-intensity X-ray beam supports measurements of areas as small as $10 \times 10 \mu\text{m}^2$, and allowed us to see fluctuations in collected charge over the entire area of the detector in a reasonable time. The IR microscopy system allows for 3D visualization of Te inclusions and other extended defects. In this paper, we describe the experimental techniques used in our measurements and typical results obtained from CZT samples produced by different suppliers.*

Keywords: CdZnTe; CZT detectors; defects in CdZnTe.

Introduction

CdZnTe (CZT) nuclear radiation detectors are advanced sensors that utilize innovative technologies based on II-VI wide band-gap semiconductor crystals and microelectronic circuitry [1-4]. They open opportunities for field deployment of compact, room-temperature operating solid-state detectors that provide accurate identification of potential radiological threats and timely awareness to both the civilian and military communities.

Solid-state radiation detectors fabricated from wide band-gap crystals represent an emerging technology that requires high-quality, uniform materials that possess relatively few defects. Despite major progress, materials deficiencies still exist for the leading candidate materials; these shortcomings limit the performance of today's gamma-ray spectrometers. Among the candidate materials, CZT is the most promising; however, its crystallinity and uniformity are not adequate except for small and somewhat inefficient devices.

To better understand the material-related problems and propose innovative solutions, we are using the X-ray beams at the National Synchrotron Light Source (NSLS) and other experimental techniques available at Brookhaven National Laboratory (BNL) to characterize CZT crystals and devices. We developed a dedicated end-station at the NSLS's beamline X27B and an infrared (IR) transmission microscopy system that allows for 3D visualization of Te inclusions, crystal defects, and correlations with detector response. A special microprobe arrangement is required for such measurements, which can be provided by the highly collimated high-intensity X-ray beams generated from Synchrotron Radiation (SR). This beam supports measurements of areas as small as $10 \times 10 \mu\text{m}^2$, and allows us to see fluctuations in collected charge over the entire area of the detector in a reasonable time. Further, we can employ other techniques (e.g, X-ray Diffraction Topography (XDT)) to assess the degree of crystalline perfection of the CZT and its relationship to detector performance.

Experimental techniques

Micro-scale Detector Mapping

The NSLS generates very bright synchrotron beams that can be collimated and monochromized in a wide energy range up to 100 keV. We constructed an apparatus and installed it in one of such beamlines for detailed investigation of a detector's performance. The set up (Fig. 1) consists of a double-slit collimator producing a $10 \times 10 \mu\text{m}^2$ beam, a precision translation stage on which we mounted CZT samples perpendicular to the incident beam, and a low-noise signal processing system [5,6].

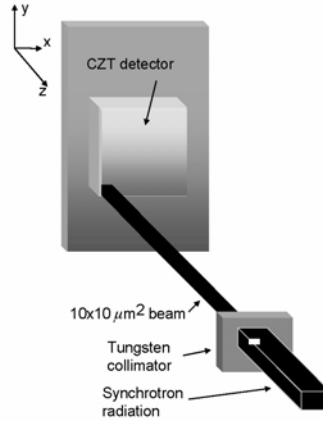


Fig. 1. Experimental set-up for the micro-scale mapping of CZT detectors.

An X-Y raster scan of the area of the detector is acquired automatically. For each position of the X-ray beam, pulse-height spectra are taken and analyzed. All the associated information such as pulse height, photopeak position, and the full width at half maximum (FWHM) are stored as a data file. The high brightness of the source facilitated the acquisition of good statistics in seconds; accordingly, a raster scan of a $1.0 \times 0.5 \text{ mm}^2$ CZT detector area was obtained within a few hours. Fig. 2(a) is an example of an X-ray map we obtained, wherein the dark regions correspond to areas of the detector where collection efficiency is affected by crystal defects.

IR microscopy

The IR transmission microscopy system comprises a large field-of-view (FOV) microscope objective, a CCD camera, motorized X-Y-Z translation stages, and a light source coupled with a wide-beam condenser for illuminating the samples [7]. The CCD camera has a $7.8 \times 10.6 \text{ mm}^2$ sensor area consisting of 2208×3000 pixels, each of $3.5 \times 3.5 \mu\text{m}^2$. The system can perform a one-, two-, or three-dimensional raster scan of a CZT crystal. At each XYZ position, an image of the area is taken and saved, and then the translation stages move the sample to the next position where this is repeated, and so on. The imaging setup allowed us to acquire stacks of images, each focused at a different depth of the crystal. An iterative algorithm was developed to identify inclusions and evaluate their sizes. CZT crystals are transparent to infrared light; however, using long wavelength light limits the feature's minimum detectable size to $\sim 1 \mu\text{m}$. In the IR images, Te inclusions larger than $10 \mu\text{m}$ are seen as relatively sharp objects with triangular or diamond-like shapes depending on crystal's orientation and the illumination. As an example, Fig. 2(b) shows an IR image of the same $1.0 \times 0.5 \text{ mm}^2$ area of the same detector used to generate X-ray map in Fig. 2(a). Correlations between dark spots in the X-ray map and Te inclusions in the IR image are clearly seen.

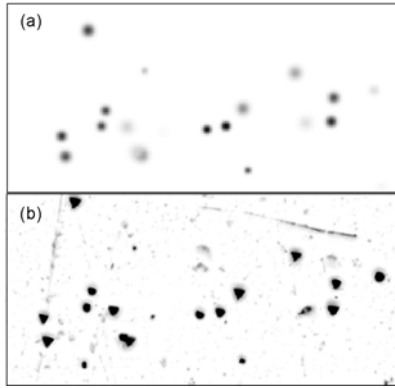


Fig. 2. (a) An x-ray map of a $1.0 \times 0.5 \text{ mm}^2$ area of CZT detector; (b) A combined IR image of the same area of the detector.

White X-ray Diffraction Topography (WXDT)

If a white beam is employed, rather than a monochromatic beam, then the diffracted beams from each point of the crystal can be observed, with different diffractions at different solid angles around the crystal. The Bragg law is applied simultaneously to each point of the crystal to denote the correct x-ray wavelength. The information gathered from this measurement reveals the number of domains and their distribution in the crystal. WXDT measurements were taken to investigate more systematically the origins of the crystal mosaicity that can supply information about the distribution of defects and strains in bulk CZT crystals. Fig. 3 shows the setup we employed for this experiment. The crystal is scanned across the $22 \times 0.2 \text{ mm}^2$ x-ray beam set by x-y slits. The information is recorded on a $20 \times 25 \text{ cm}^2$ imaging plate with a resolution of $50 \mu\text{m}$. Only a few orders of diffractions are recorded.

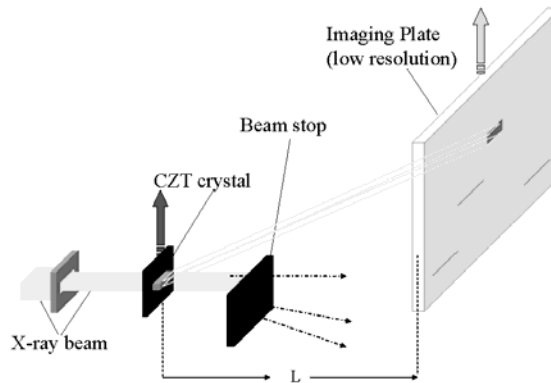


Fig. 3. Set up for obtaining WXDT measurements from a crystal. The distance L between imaging plate and CZT crystal is 153 cm. The imaging plate is scanned in the same direction at the same speed as that of the crystal as it is scanned across the beam.

By using special photographic films a resolution of a few micrometers can be achieved. The imaging plate is scanned in the same direction at the same speed as that of the crystal as it is scanned across the beam. Fig. 4 shows the topography of a $27 \times 27 \text{ mm}^2$ CZT sample, in which several domains are distinguishable. In this measurement, the white beam was ranged from 50 keV to 200 keV. The high flux of the beam allowed us to work in the transmission mode, with CZT crystals that were several millimeters thick. Scanning the CZT crystals is very rapid; the measurements are completed in a few seconds. Hence, batches of CZT crystals can be screened quickly. We used this methodology to ensure that the CZT samples are all single crystals.

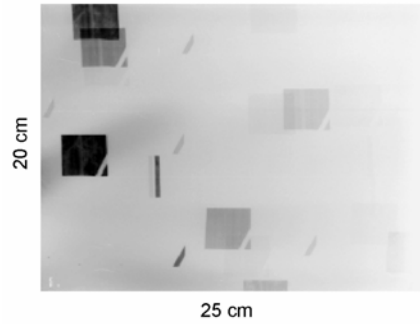


Fig. 4. WXDT image of a 27x27x2mm³ CZT crystal. This crystal presents three domains, and it is possible to distinguish the three different diffracted images.

Etch-pit density (EPD) analysis:

We employed chemical etching to reveal the etch pits in rejected CZT crystals. The principal purpose was to seek correlations between EPDs and the poor performance of some radiation detectors [8]. In the past, chemical etching methods have been applied to identify the presence of the crystallographic dislocations and subgrain boundaries in CdTe and CdZnTe crystals. Several different etchants have been proposed for CdTe family materials, in particular a Nakagawa solution is commonly used for studying dislocations in CZT crystals. Etch pits are formed at the exit points of dislocations on the surface, which give a direct measure of dislocation densities. The pits have certain depths that may give indication of the general direction of the dislocation lines. Each sample was polished and etched several times to reveal dislocations at different depths. We used 5- μ m grit Al₂O₃ abrasive paper to lap the samples prior to fine polishing and chemical etching in 2% Bromine-Methanol (B-M) solution for 5 minutes. The latter steps are very important for removing the surface layers damaged by mechanical lapping. After polishing, the samples were etched with Nakagawa solution for 2-3 minutes and then dipped in B-M solution for 1 second to remove the black surface layer. Finally, the samples are dried using nitrogen gas. The etched surfaces were investigated under the IR microscope system in both transmission and reflection light modes.

Fig. 5 shows a reflection photograph of the etched surface of a 5x12 mm² area of a CZT crystal. The individual etch pits are barely seen on this spatial scale, but many of them are arranged in the linear patterns (walls) crossing the CZT sample. A single etch pit reveals an exit point of a dislocation while their linear associations represent the dislocation walls emerging on the crystal. Such walls (also called low-angle boundaries) are formed as a result of the dislocation polygonization occurring during the annealing.

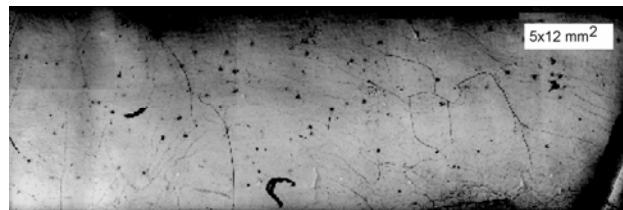


Fig. 5. A reflection photograph of the etched surface of one representative crystal. Etch pits are arranged in the linear patterns (walls) crossing the CZT sample.

Conclusions

We employed several experimental techniques to investigate CZT crystals grown by commercial vendors. Our results reveal a correlation between Te inclusions and dislocations and areas with reduced charge collection efficiency. The structural defects observed in the map can be related to some features observed in the WXDT image, but measurements with higher resolutions are needed to reveal structural defects, such as lattice distortion and subgrain boundaries.

Acknowledgment

This work was supported by the Defense Threat Reduction Agency and U.S. Department of Energy, Office of Nonproliferation Research and Development, NA-22. The manuscript has been authored by Brookhaven Science Associates, LLC under Contract No. DE-AC02-98CH1-886 with the U.S. Department of Energy.

References

1. R. B. James, T. E. Schlesinger, J. C. Lund and M. Schieber, "*Cadmium Zinc Telluride Spectrometers for Gamma and X-Ray Applications*", in *Semiconductors for Room Temperature Nuclear Detector Applications*, Vol. 43, edited by R. B. James and T. E. Schlesinger (Academic Press, New York, 1995), p. 334.
2. C. Szeles and E. E. Eissler, "*Current issues of High-pressure Bridgman growth of semi-insulating CdZnTe*", in *Semiconductors for Room Temperature Radiation Detector Applications II*, Vol. 487, edited by R. B. James, T. E. Schlesinger, P. Siffert, W. Dusi, M. R. Squillante, M. O'Connell and M. Cuzin (Materials Research Society, Pittsburgh, PA, 1998), pp. 3-12.
3. J. R. Heffelfinger, D. L. Medlin, and R. B. James, "*Analysis of Grain Boundaries, Twin Boundaries and Te Inclusions in Cadmium Zinc Telluride Grown by High-Pressure Bridgman Method*", in *Semiconductors for Room Temperature Radiation Detector Applications II*, Vol. 487, edited by R. B. James, T. E. Schlesinger, P. Siffert, W. Dusi, M. R. Squillante, M. O'Connell and M. Cuzin (Materials Research Society, Pittsburgh, PA, 1998), p. 33.
4. C. Szeles, S. E. Cameron, J.-O. Ndap, W. C. Chalmers, "*Advances in the crystal growth of semi-insulating CdZnTe for radiation detector applications*", *IEEE Trans. Nucl. Sci.* 49, no. 5, pp. 2535-2540, 2002.
5. G. A. Carini, A. E. Bolotnikov, G. S. Camarda, G. W. Wright, L. Li, and R. B. James, "*Effect of Te inclusions on the performance of CdZnTe detectors*", *Appl. Phys. Lett.* 88, p. 143515, 2006.
6. G. S. Camarda, A. E. Bolotnikov, G. A. Carini, and R. B. James, "*Effects of Tellurium Inclusions on charge collection in CZT Nuclear Radiation Detectors*", in *Countering Nuclear and Radiological Terrorism*, edited by S. Aprkryan and D. Diamond, Springer, 2006, pp. 199-207.
7. A. E. Bolotnikov, G. S. Camarda, G. A. Carini, Y. Cui, K. T. Kohman, L. Li, M. B. Salomon, and R. B. James, "*Performance-limiting Defects in CdZnTe Detectors*", *IEEE Trans. Nucl. Sci.* 54, [no. 4](#), pp. 821-827, 2007.
8. A. Hossain, A. E. Bolotnikov, G. C. Camarda, Y. Cui, G. Yang, and R. B. James, "*Defects in Cadmium Zinc Telluride Crystals revealed by etch pit distributions*", *J. Crystal Growth* 310, Issue 21, pp. 4493-4498, 2008.